Int J Adv Manuf Technol (2016) 84:621–630
DOI 10.1007/s00170-015-7707-9

ORIGINAL ARTICLE

A study of computing accuracy of calibrating cutting force coefficients and run-out parameters in flat-end milling

Dongliang Zhang[1] · **Rong Mo**[1] · **Zhingyong Chang**[1] · **Huibin Sun**[1] · **Chunlei Li**[1]

Received: 1 April 2015 / Accepted: 7 August 2015 / Published online: 29 August 2015

Abstract It is well known that the presence of cutter run-out has a significant effect upon the instantaneous uncut chip thickness through redistributing it and thereby contributes to the irregular change on the cutting forces in one tooth periods. In this paper, in order to avoid the numerical oscillations from differential model and to eliminate the influence of the ill-posed problem in calibration, a new approach to calibrate the cutter radial run-out parameters from the continuous cutting force model with constant cutting coefficients was proposed. Through analyzing the influence of the ill-posed problem in calibration of the tangential and radial cutting force coefficients, the corresponding solution method was proposed to enhance the calculation stability and to get a useful and stable solution. The cutting force coefficient matrix was optimized by incorporating the average cutting information in x and y directions based on the least square method. Furthermore, through numerical simulation and experimental results, the validity of the calibration approach is demonstrated.

Keywords Run-out parameters · Cutting force · Flat-end milling · Calibration · Cutting force coefficients

1 Introduction

An accurate cutting force prediction model is the key to calibration of cutting force coefficients, essential for analysis of machining process, the optimization of federate, the prediction of surface quality, and the control of vibrations. To ensure accuracy, extensive research efforts are sacrificed to establish a reliable cutting force prediction model. The earliest cutting force prediction model was provided by Koenigsberger and Sabberw, and the cutting forces are assumed to be directly proportional to the chip cross-sectional area, and the proportional coefficients, i.e., cutting force coefficients may be assumed to be constants depending on the cutting conditions and material properties [1]. With this idea in mind, Kline et al. presented a numerical model for the prediction of cutting forces in end milling, where the cutting forces were assumed to be directly proportional to the uncut chip thickness, and the cutting force coefficients were constants [2].

Actually, the effect of run-out was ignored in some studies, although the instantaneous uncut chip thickness is redistributed by the presence of cutter run-out [3, 4]. More accurate milling force models have been proposed in consideration of the influence of cutter run-out. Liang and Wang formulated and analyzed the effect of cutter run-out on the milling force in the frequency domain, and the magnitude and angular location of cutter run-out were calibrated with the Fourier series coefficients of cutting forces [5]. Wang presented an approach for the identification of cutter run-out through two cutting tests, and the milling force is synthesized through convolution [6]. The methods mentioned above are based on the Fourier analysis of these force components revealing the effects of offset geometry.

It is important to note that there are some debates in the academia about the identification of the cutting force coefficients. Melkote and Endres assumed that the usage of constant cutting force coefficients might lose the accuracy of the prediction at peak values of the instantaneous uncut chip thickness, during tool entry and exit periods [7].

✉ Rong Mo
morong@nwpu.edu.cn

[1] Northwestern Polytechnical University, Xi'an, China

But, some studies showed that the usage of constant coefficients can not only simplify the procedure of the calibration but make the results precise [8–10]. Cutting forces are predicted by superposing the cutting force of discrete sliced elements from the bottom of the flute toward the final axial depth of cut in many studies [11, 12]. And, the numerical oscillations on the cutting force waveforms can be caused, which maybe lead to faulty simulation of cutting vibration [3]. This is why the cutting force model is established based on the integral calculation method in this paper.

In this paper, we proposed the method to identify the cutter run-out parameters from the continuous cutting force model with constant cutting coefficients in the flat-end milling. Firstly, the calculation formulas for calibrating these values are deduced based on the least square method. Then, the coefficient matrixes are reconstructed to obtain the stable solution. At last, based on simulation and experimental results, the stability and the accuracy of the calculation method are demonstrated.

The main features of the approach given in this paper can be summarized as follows:

1. To avoid the numerical oscillations from differential model, the run-out parameters were determined from the continuous cutting force model with constant cutting coefficients in this paper.
2. To eliminate or reduce the influence of the ill-posed problem in calibration of the tangential and radial cutting force coefficients, the causes of this problem was analyzed and the solution method was proposed to enhance the calculation stability and to get a useful and stable solution.

2 Milling forces with cutter run-out

2.1 Basic cutting force model

An end milling process is illustrated in Fig. 1, with a helix angle of β, diameter of R_D, N number of tool teeth, the axial cutting depth of a_p, and the radial cutting depth of a_e. When the milling cutter comes into contact with the workpiece, the cutting force can appear. So the angular position $\phi_{c,i,j}(z)$ for the element of cutting edge i at axial depth of cut z is expressed as follows:

$$\phi_{c,i,j}(z) = \phi_j - (i-1)\frac{2\pi}{N} - k_\beta z \tag{1}$$

where $k_\beta = \frac{\tan(\beta)}{R_D}$ and ϕ_j is the cutter rotation angle, j =1, 2,⋯,n , n is the number of sampling cutter rotation angle position.

The cutting forces applied on the element of cutting edge i at the angular position ϕ_j with height dz, can be divided into components: tangential $dF_{t,i,j}$, radial $dF_{r,i,j}$, and axial $dF_{a,i,j}$. These are expressed similar to Eq. (2) as follows:

$$\begin{aligned} dF_{t,i,j} &= \left(K_{tc}h_{i,j}(z) + K_{te}\right)dz \\ dF_{r,i,j} &= \left(K_{rc}h_{i,j}(z) + K_{re}\right)dz \\ dF_{a,i,j} &= \left(K_{ac}h_{i,j}(z) + K_{ae}\right)dz \end{aligned} \tag{2}$$

The $h_{i,j}(z)$ is the instantaneous uncut chip thickness associated with the element of cutting edge i at the ϕ_j. Cutting force is divided into shearing force caused by shearing in the shear zone, and blade force derived from flank surface friction of the cutting edge. The shearing force can be expressed as the product of tangential force coefficient K_{tc}, radial force coefficient K_{rc}, axial force coefficient K_{ac}, and the shear area; the blade force can be expressed as the product of tangential blade force coefficient K_{te}, radial blade force coefficient K_{re}, axial blade force coefficient K_{ae}, and cutting width.

The elemental forces are resolved into feed (x), normal (y), and axial (z) direction using the transformation as follows:

$$\begin{cases} dF_{x,i,j} = -dF_{t,i,j}\cos\left(\phi_{c,j} - k_\beta z\right) - dF_{r,i,j}\sin\left(\phi_{c,j} - k_\beta z\right) \\ dF_{y,i,j} = dF_{t,i,j}\sin\left(\phi_{c,j} - k_\beta z\right) - dF_{r,i,j}\cos\left(\phi_{c,j} - k_\beta z\right) \\ dF_{z,i,j} = dF_{a,i,j} \end{cases} \tag{3}$$

The differential cutting forces are integrated analytically along the in-cut portion of the cutting edge i to obtain the total cutting force produced by the blade as follows:

$$\begin{aligned} F_{x,i} &= \int_{z_{1,i,j}}^{z_{2,i,j}} dF_{x,i,j}dz \\ F_{y,i} &= \int_{z_{1,i,j}}^{z_{2,i,j}} dF_{y,i,j}dz \\ F_{z,i} &= \int_{z_{1,i,j}}^{z_{2,i,j}} dF_{z,i,j}dz \end{aligned} \tag{4}$$

where $z_{1,i,j}$ and $z_{2,i,j}$ are the lower and upper axial engagement limits of the in-cut portion of the blade i at the angular position ϕ_j.

2.2 Instantaneous uncut chip thickness model with cutter radial run-out

According to the analysis of the movement of the cutting edge element, the instantaneous uncut chip thickness should be calculated accurately with cutter radial run-out. Figure 2 shows the radial run-out of the end milling process. Under the influence of cutter run-out, the rotation radius of an arbitrary element of cutting edge i with respect to axial position z can be expressed as

$$R_i(z) = R_D + \rho\cos\left(\lambda - k_\beta z - (i-1)\frac{2\pi}{N}\right), \cdot i = 1, 2, \cdots, N \tag{5}$$

where ρ is the run-out offset, λ is defined as the location angle measured clockwise from the offset direction to the nearest tooth tip that corresponds to tooth 1.

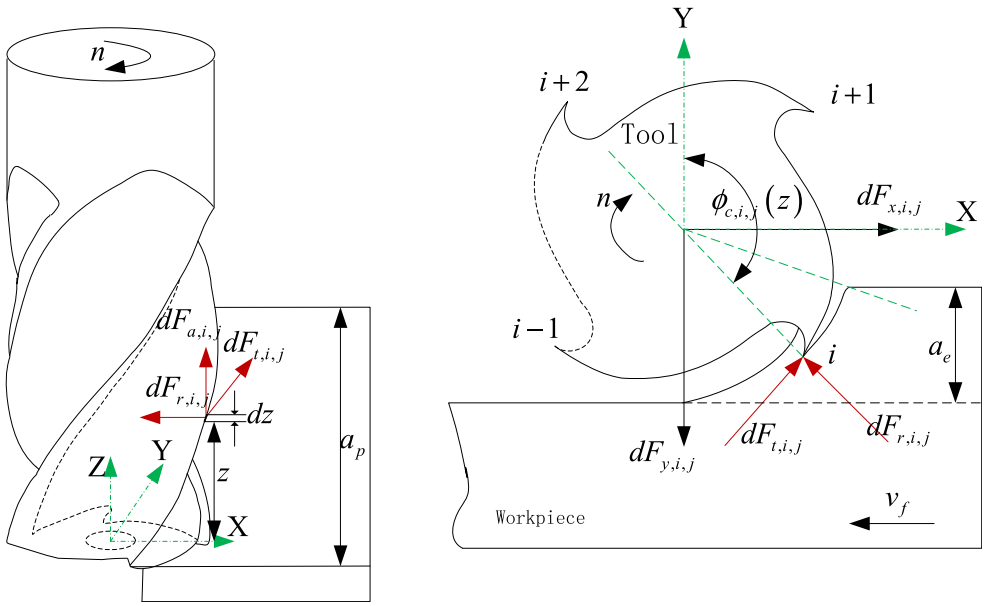

Fig. 1 Force analysis in a workpiece cut by an end milling

The instantaneous uncut chip thickness $h_i(\phi,z)$ of an arbitrary element of cutting edge i with the circular tooth path approximation can be given as [2, 13].

$$h_i = m_i f_z \sin\left(\phi_j - k_\beta z\right) + R_i(z) - R_{i-m_i}(z) \tag{6}$$

where the m_i means that the current tooth i is removing the material left by the $m_{i\text{th}}$ previous tooth with the feed f_z per tooth.

Substituting Eq. (5) into Eqs. (6) and (7) is obtained as follows.

$$h_i(\phi,z) = m_i f_z \sin\left(\phi_j - k_\beta z\right) + 2\rho \sin\left(\lambda - k_\beta z - \frac{\pi}{N}(2i - m_i - 2)\right)\sin\left(\frac{m_i \pi}{N}\right) \tag{7}$$

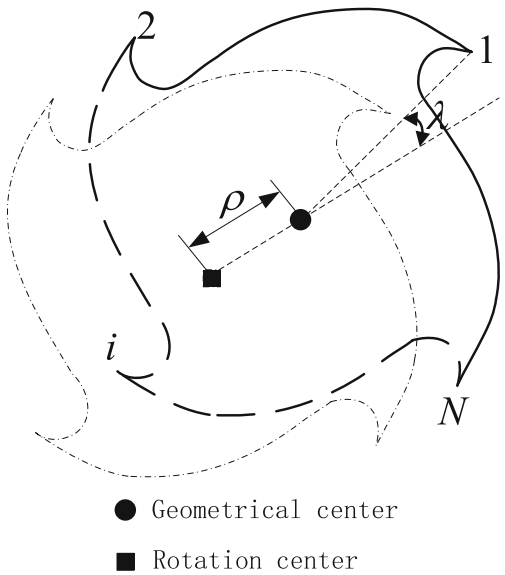

Fig. 2 Geometry of the cutter run-out

From the preceding discussion, the cutting path of an arbitrary element of cutting edge is influenced by the cutter radial run-out, so that the current cutting surface may not be left by the last cutting edge. So, the solution of the m_i in the Eq. (8) is very complex essentially, which depends on the helical angle, the immersion angle, the run-out parameters and the axial cutting depth. Obviously, the m_i could not be solved if the run-out parameters are unknown. In order to deal with this paradox and acquire the results fitting the experimental results well, the m_i is commonly assumed to be 1, and this means that cutting surface is supposed to be left by the last cutting edge [12, 14]. So, the instantaneous uncut chip thickness $h_i(\phi,z)$ can be expressed that it consists of two parts as shown in Eq. (8).

$$h_i\left(\phi_{c,i,j}(z)\right) = h_{i,1}\left(\phi_{c,i,j}(z)\right) + h_{i,2}\left(\phi_{c,i,j}(z)\right) \tag{8}$$

where

$$h_{i,1}\left(\phi_{c,i,j}(z)\right) = f_t \sin\left(\phi_{c,i,j}(z)\right)$$
$$h_{i,2}(z) = 2\rho \sin\left(\lambda - k_\beta z - \frac{\pi}{N}(2i-3)\right)\sin\left(\frac{\pi}{N}\right)$$

2.3 Pro-process for calculating the cutting-force coefficients and the cutter run-out parameters

At the shown in Fig. 1, the total cutting force produced by the cutting edge is calculated by integrating the differential cutting forces. By combining Eqs. (4) and (5), the sum of all X, Y, and Z forces of the cutting edge elements with respect to the cutter rotation angular can be obtained as shown in Eq. (9). The lower and upper axial engagement limits of the in-cut portion z_1 and z_2 corresponding the cutter rotation angle can be solved by the methods in preterit articles [15, 16].

$$\begin{cases} F_{x,i,j} = \int_{z_{i,1}}^{z_{i,2}} \left[-K_{tc}h_i\cos\left(\phi_{c,i,j}(z)\right)-K_{rc}h_i\sin\left(\phi_{c,i,j}(z)\right)-K_{te}\cos\left(\phi_{c,i,j}(z)\right)-K_{re}\sin\left(\phi_{c,i,j}(z)\right)\right]dz \\ F_{y,i,j} = \int_{z_{i,1}}^{z_{i,2}} \left[K_{tc}h_i\sin\left(\phi_{c,i,j}(z)\right)-K_{rc}h_i\cos\left(\phi_{c,i,j}(z)\right)-K_{te}\sin\left(\phi_{c,i,j}(z)\right)-K_{re}\cos\left(\phi_{c,i,j}(z)\right)\right]dz \\ F_{z,i,j} = \int_{z_{i,1}}^{z_{i,2}} [K_{ac}h_i + K_{ae}]dz \end{cases} \quad (9)$$

Note that $\sum_{i=1}^{n}\sin\left(a+\frac{2\pi i}{n}\right)=\sum_{i=1}^{n}\cos\left(a+\frac{2\pi i}{n}\right)=0$, where a is an arbitrary constant. So, $\sum_{i=1}^{N} h_{i,2}(z) = \sum_{i=1}^{N}\left(2\rho\sin\left(\lambda-k_\beta z-\frac{\pi}{N}(2i-3)\right)\sin\left(\frac{\pi}{N}\right)\right)=0$ and $\sum_{i=1}^{N} h_{i,1}(\phi_{c,i,j}(z)) = \sum_{i=1}^{N} h_{i,1}=Nf_t\sin\left(\phi_{c,j}-k_\beta z\right)$.

Through substituting the instantaneous uncut chip thickness $h_i(\phi,z)$ into the Eq. (9) and accumulating the cutting forces of different cutting edges, we can obtain the Eq. (10)

$$\begin{cases} \sum_{i=1}^{N} F_{x,i}\left(\phi_{c,i,j}(z)\right)/N = -K_{tc}C_{1,i,j}-K_{rc}S_{1,i,j}-K_{te}C_{2,i,j}-K_{re}S_{2,i,j} \\ \sum_{i=1}^{N} F_{y,i}\left(\phi_{c,i,j}(z)\right)/N = K_{tc}S_{1,i,j}-K_{rc}C_{1,i,j}+K_{te}S_{2,i,j}+K_{re}C_{2,i,j} \\ \sum_{i=1}^{N} F_{z,i}\left(\phi_{c,i,j}(z)\right)/N = f_tS_{2,i,j}K_{ac}+K_{ae} \end{cases} \quad (10)$$

$$S_{1,i,j} = \int_{z_{1,i,j}}^{z_{2,i,j}} \sin\left(\phi_{c,i,j}(z)\right)h_{i,1}\left(\phi_{c,i,j}(z)\right)dz$$

$$C_{1,i,j} = \int_{z_{1,i,j}}^{z_{2i,j}} \cos\left(\phi_{c,i,j}(z)\right)h_{i,1}\left(\phi_{c,i,j}(z)\right)dz$$

$$S_{2,i,j} = \int_{z_{1,i,j}}^{z_{2,i,j}} \sin\left(\phi_{c,i,j}(z)\right)dz$$

$$C_{2,i,j} = \int_{z_{1,i,j}}^{z_{2,i,j}} \cos\left(\phi_{c,i,j}(z)\right)dz$$

By subtracting average cutting forces from instantaneous cutting force, the cutter run-out parameters can be separated from the instantaneous uncut chip thickness as shown in Eq. (11).

$$\begin{cases} F_{x,i,j}-\sum_{i=1}^{N} F_{x,i,j}\Big/N = 2\sin\left(\frac{\pi}{N}\right)\left(\left(-K_{tc}A_{1,i,j}-K_{rc}A_{2,i,j}\right)(\rho\sin\alpha_i) + \left(-K_{te}A_{3,i,j}-K_{re}A_{4,i,j}\right)(\rho\cos\alpha_i)\right) \\ F_{y,i,j}-\sum_{i=1}^{N} F_{y,i,j}\Big/N = 2\sin\left(\frac{\pi}{N}\right)\left(\left(K_{tc}A_{2,i,j}-K_{rc}A_{1,i,j}\right)(\rho\sin\alpha_i) + \left(K_{te}A_{4,i,j}-K_{re}A_{3,i,j}\right)(\rho\cos\alpha_i)\right) \end{cases} \quad (11)$$

$$\alpha_i = \lambda-\frac{\pi}{N}(2i-3)$$

$$\begin{aligned} A_{1,i,j} &= M_{1,i,j}\sin\left(\phi_{c,i,j}(z)\right) + M_{2,i,j}\sin\left(\phi_{c,i,j}(z)\right) \\ A_{2,i,j} &= M_{2,i,j}\sin\left(\phi_{c,i,j}(z)\right)-M_{1,i,j}\cos\left(\phi_{c,i,j}(z)\right) \\ A_{3,i,j} &= -M_{3,i,j}\sin\left(\phi_{c,i,j}(z)\right)-M_{1,i,j}\cos\left(\phi_{c,i,j}(z)\right) \\ A_{4,i,j} &= -M_{1,i,j}\sin\left(\phi_{c,i,j}(z)\right) + M_{3,i,j}\cos\left(\phi_{c,i,j}(z)\right) \end{aligned}$$

$$M_{1,i,j} = \int_{z_{1,i,j}}^{z_{2,i,j}} \sin\left(2k_\beta z\right)dz$$

$$M_{2,i,j} = \int_{z_{1,i,j}}^{z_{2,i,j}} \left(1+\cos\left(2k_\beta z\right)\right)dz$$

$$M_{3,i,j} = \int_{z_{i,1}}^{z_{i,2}} \left(1-\cos\left(2k_\beta z\right)\right)dz$$

2.4 The analysis of ill-posed problem about calibrating the coefficients

The formula for determining cutting-force coefficients can be derived easily from the Eq. (10). The solution problem of the

Table 1 Three-axis milling experiment parameters

Test no.	Milling type	Radial depth of cut a_e/mm	Axial depth of a_p/mm	Feed per tooth f_z/(mm per tooth)	Rotation speed /(r·min^{-1})
1	Down	3	3	0.04	6000
2	Down	3	2	0.05	6000
3	Down	2	3	0.06	6000
4	Up	3	3	0.02	6000
5	Up	3	2	0.03	6000
6	Up	2	3	0.04	6000

cutting force coefficients is a parameter identification problem, and the cutting force coefficients K_{tc}, K_{rc} and the blade force coefficients K_{te}, K_{re} can be identified through least-square method as shown in Eq. (12).

$$\begin{bmatrix} K_{tc} \\ K_{rc} \\ K_{te} \\ K_{re} \end{bmatrix} = \left(\mathrm{V}_{x,i}{}^{T}\cdot\mathrm{V}_{x,i}\right)^{-1}\cdot V_{x,i}{}^{T}\cdot \begin{bmatrix} \sum_{i=1}^{N} F_{x,i,1}/N \\ \sum_{i=1}^{N} F_{x,i,2}/N \\ \vdots \\ \sum_{i=1}^{N} F_{x,i,j}/N \\ \vdots \\ \sum_{i=1}^{N} F_{x,i,n}/N \end{bmatrix} \tag{12}$$

where

$$\mathrm{V}_{x,i} = \begin{bmatrix} -C_{1,i,1} & -S_{1,i,1} & -C_{2,i,1} & -S_{2,i,1} & 0 & 0 \\ -C_{1,i,2} & -S_{1,i,2} & -C_{2,i,2} & -S_{2,i,2} & 0 & 0 \\ \vdots & \vdots & \vdots & \vdots & \vdots & \vdots \\ -C_{1,i,j} & -S_{1,i,j} & -C_{2,i,2} & -S_{2,i,j} & 0 & 0 \\ \vdots & \vdots & \vdots & \vdots & \vdots & \vdots \\ -C_{1,i,n} & -S_{1,i,n} & -C_{2,i,n} & -S_{2,i,n} & 0 & 0 \end{bmatrix}$$

Actually, the order of magnitude of the condition number of coefficients matrix $\mathrm{V}_{x,i}$ is around 10^3 in practical experiments. This implies that the coefficients matrix $\mathrm{V}_{x,i}$ is ill-conditioned, and the computed solution is potentially very sensitive to perturbations of the data. Usually, this phenomenon is called the ill-posed problem. The main impact on the accuracy in calibration with the ill-posed problem is that it is essentially underdetermined due to the cluster of small singular values of the coefficient matrix. Therefore, it is necessary to contain more information about the conceivable solution in order to

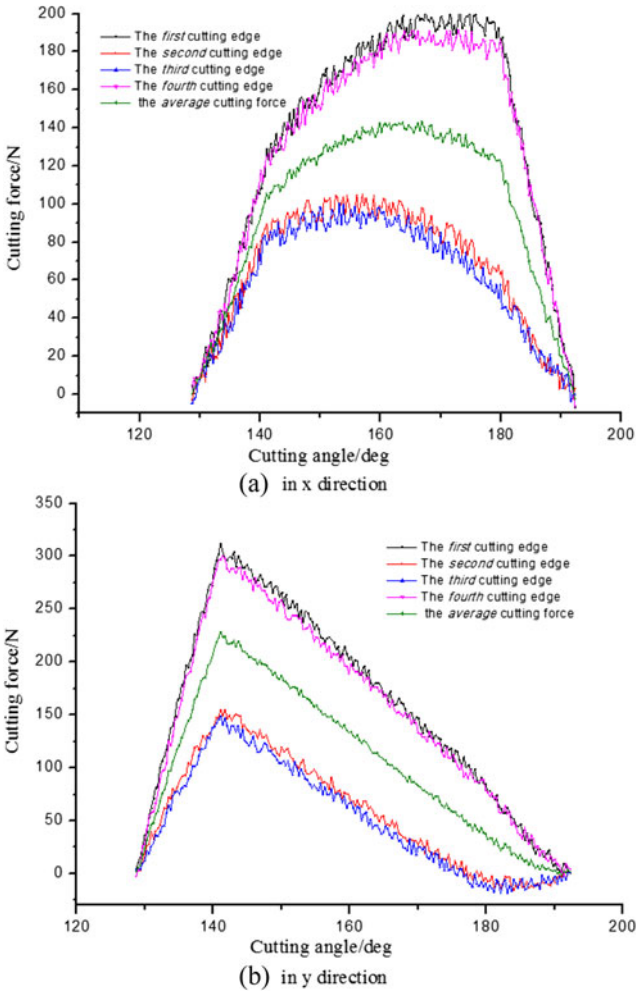

Fig. 3 **a** The cutting forces from different cutting edges and the average cutting force in *x* direction of test no. 1. **b** The cutting forces from different cutting edges and the average cutting force in *y* direction of test no. 1

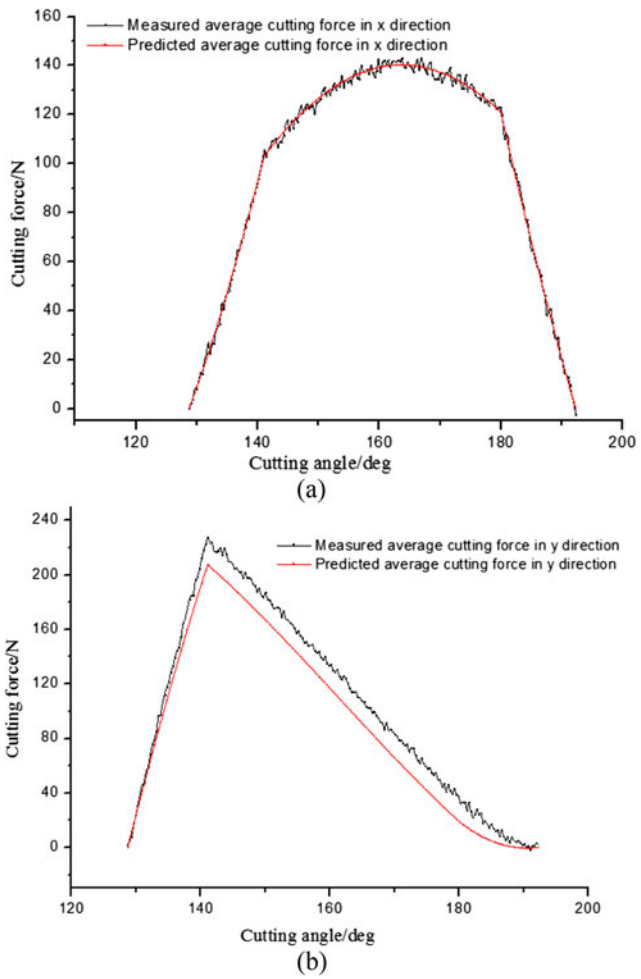

Fig. 4 **a** The measured and predicted average cutting forces in *x* direction of test no. 1. **b** The measured and predicted average cutting forces in *x* direction of test no. 1

enhance the calculation stability and get a useful and stable solution. This is the purpose of study in this paper. In next section, the method to improve the calculation stability by solving the ill-posed problem of coefficients matrix $V_{x,i}$ will be discussed in detail.

Based on the least-square method, the axial cutting force coefficients K_{ac} and the axial blade force coefficients K_{ae} can be derived from Eq. (13).

$$\begin{bmatrix} K_{ac} \\ K_{ae} \end{bmatrix} = \left(V_{z,i}{}^{T} \cdot V_{z,i}\right)^{-1} \cdot V_{z,i}{}^{T} \cdot \begin{bmatrix} F_{z,i,1} \\ F_{z,i,2} \\ \vdots \\ F_{z,i,j} \\ \vdots \\ F_{z,i,n} \end{bmatrix} \tag{13}$$

where

$$V_{z,i} = \begin{bmatrix} P_{i,1} + Q_{i,1} & R_{i,1} \\ P_{i,2} + Q_{i,2} & R_{i,2} \\ \vdots & \vdots \\ P_{i,j} + Q_{i,j} & R_{i,j} \\ \vdots & \vdots \\ P_{i,n} + Q_{i,n} & R_{i,n} \end{bmatrix}, \cdot \quad \begin{cases} P_{i,j} = f_t \dfrac{1}{k_\beta} S_{2,i,j} \\ Q_{i,j} = 2\rho \sin\left(\dfrac{\pi}{N}\right) \displaystyle\int_{z_{1,i,j}}^{z_{2,i,j}} \sin\left(\lambda - k_\beta z - \frac{\pi}{N}(2i-3)\right) dz \\ R_{i,j} = \displaystyle\int_{z_{1,i,j}}^{z_{2,i,j}} dz \end{cases}$$

It is noteworthy that the order of magnitude of the condition number of coefficients matrix $V_{z,i}$ is much less than coefficients matrix $V_{x,i}$. Thus, the solution is not sensitive to perturbations of the data.

When the cutting force coefficients and the blade force coefficients are known, the run-out parameters can be determined as shown in Eq. (14).

$$\begin{bmatrix} a_i \\ b_i \end{bmatrix} = \left(W^T \cdot W\right)^{-1} \cdot W^T \cdot \begin{bmatrix} F_{x,i,1} - \sum_{i=1}^{N} F_{x,i,1}/N \\ F_{x,i,2} - \sum_{i=1}^{N} F_{x,i,2}/N \\ \vdots \\ F_{x,i,j} - \sum_{i=1}^{N} F_{x,i,j}/N \\ \vdots \\ F_{x,i,n} - \sum_{i=1}^{N} F_{x,i,n}/N \end{bmatrix} \tag{14}$$

where

$$a_i = \rho \sin\alpha_i, \cdot b_i = \rho \cos\alpha_i \quad \text{and} \quad W$$

$$= 2\sin\left(\frac{\pi}{N}\right) \begin{bmatrix} -K_{tc}A_{1,i,1} - K_{rc}A_{2,i,1} & -K_{te}A_{3,i,1} - K_{re}A_{4,i,1} \\ -K_{tc}A_{1,i,2} - K_{rc}A_{2,i,2} & -K_{te}A_{3,i,2} - K_{re}A_{4,i,2} \\ \vdots & \vdots \\ -K_{tc}A_{1,i,j} - K_{rc}A_{2,i,j} & -K_{te}A_{3,i,j} - K_{re}A_{4,i,j} \\ \vdots & \vdots \\ -K_{tc}A_{1,i,n} - K_{rc}A_{2,i,n} & -K_{te}A_{3,i,n} - K_{re}A_{4,i,n} \end{bmatrix}$$

The solving method for the run-out parameters is just similar with that for the axial cutting force coefficients K_{ac} and the axial blade force coefficients K_{ae}. The matrix W is not ill-conditioned, and we can obtain more accurate result without enhancing the calculation stability.

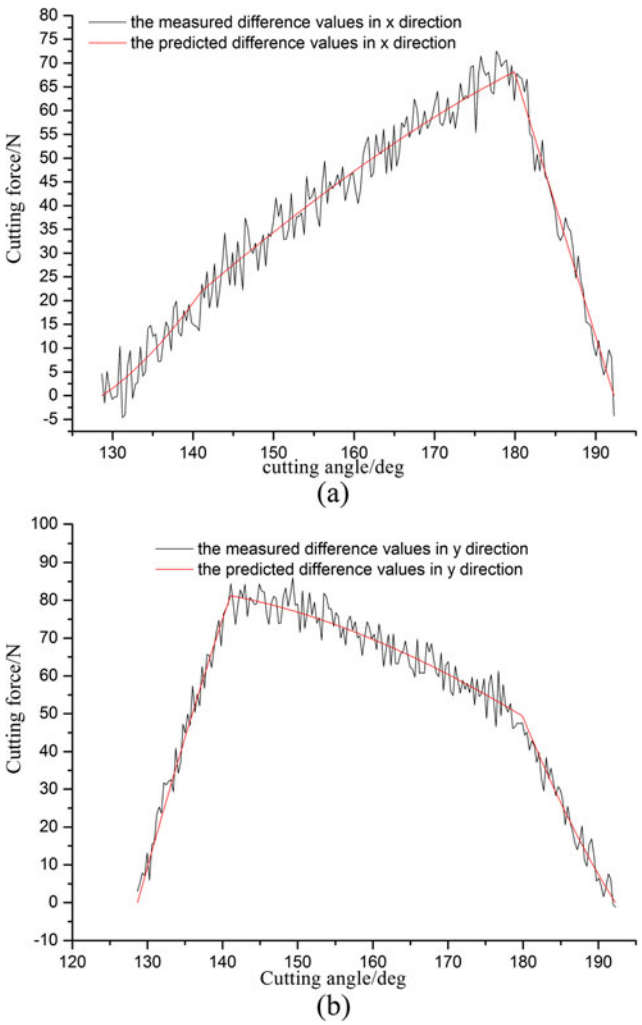

Fig. 5 **a** The measured and predicted difference values between the cutting force of the first edge and the average cutting force in *x* direction. **b** The measured and predicted difference values between the cutting force of the first edge and the average cutting force in *y* direction

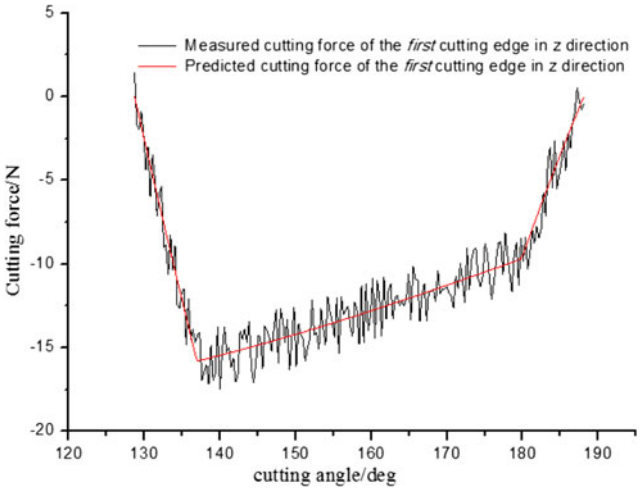

Fig. 6 The average cutting force of the first cutting edge in z direction

3 Experimental verifications

3.1 The experiment on the accuracy of calibration

In the experiment of calibrating of cutting force coefficients, ill-posed problem about calibrating the coefficients was observed as the accuracy of calibration is highly susceptible to perturbations of the cutting force signal. But, in the actual experiments, the received signal ineluctably has some distortion. In this section, the calibrating accuracy of cutting force coefficients with the signal interference was analyzed.

The validity of the proposed approach of calibrating the cutting force coefficients is implemented through a series of cutting tests on a three-axis CNC vertical milling machine. A four-fluted flat-end mill with a diameter of 8 mm and a helix angle of 30° is set up on the three-axis CNC vertical milling. The workpiece material is 45 steel and the cutting forces are measured with a KISTLER 9265B dynamometer. The cutting types and cutting conditions in the test are illustrated in Table 1.

As an example to illustrate the ill-posed problem in the calibration, the calibrating process of the test no. 1 was discussed. The cutting forces from different cutting edges and the average cutting force in x direction and in y direction of test no. 1 provided by a dynamometer can be seen in Fig. 3.

The thing to note here is that cutting angles of different edges was transformed into the cutting region of the first edge.

As mentioned above, the cutting forces signal almost always is effected by noise and interference. So, only using the Eq. (12), the accuracy of the calibration will not be satisfactory. In test no. 1, the calibration values of the cutting force coefficients K_{tc}, K_{rc} and the blade force coefficients K_{te}, K_{re} by using the Eq. (12) are 1353.538, 938.620, 35.299, and −2.2017. In fact, the condition number of coefficients matrix $V_{x,i}$ in x direction of test no. 1 is 2880.393. To illustrate the influence on the calibration accuracy, the measured and predicted average cutting forces using the above calibration values in x and in y direction of test no. 1 are shown in Fig. 4. It is obvious that the predicted results are of well conformity with the measured cutting forces in x direction. However, the fitting results are not satisfactory in y direction.

In order to find out a useful and stable solution to satisfy the fitting precision in x and y directions, it is necessary to incorporate further information about the desired solution. Thus, this paper reconstructs the Eq. (12) as shown in Eq. (15). In test no. 1, the calibration values of the cutting force coefficients K_{tc}, K_{rc} and the blade force coefficients K_{te}, K_{re} are 1502.719, 872.907, 35.214, and 3.924. In Fig. 4, we can see these predicted results coincide with the experimental very well both in x and in y directions.

$$\begin{bmatrix} K_{tc} \\ K_{rc} \\ K_{te} \\ K_{re} \end{bmatrix} = \left(\mathrm{V}_{xy,i}{}^{T}\cdot\mathrm{V}_{xy,i}\right)^{-1}\cdot V_{xy,i}{}^{T}\cdot\begin{bmatrix} \mathrm{F}_x \\ \mathrm{F}_y \end{bmatrix} \tag{15}$$

where

$$\mathrm{F}_x = \begin{bmatrix} \sum_{i=1}^{N} F_{x,i,1}/N \\ \sum_{i=1}^{N} F_{x,i,2}/N \\ \vdots \\ \sum_{i=1}^{N} F_{x,i,j}/N \\ \vdots \\ \sum_{i=1}^{N} F_{x,i,n}/N \end{bmatrix}, \quad \mathrm{F}_y = \begin{bmatrix} \sum_{i=1}^{N} F_{y,i,1}/N \\ \sum_{i=1}^{N} F_{y,i,2}/N \\ \vdots \\ \sum_{i=1}^{N} F_{y,i,j}/N \\ \vdots \\ \sum_{i=1}^{N} F_{y,i,n}/N \end{bmatrix}, \quad \mathrm{V}_{xy,i} = \begin{bmatrix} \mathrm{V}_{x,i} \\ \mathrm{V}_{y,i} \end{bmatrix}$$

Table 2 Experimental results: the identified cutting force coefficients and cutter run-out parameters

Test no.	Cutting force coefficients						Run-out parameters	
	K_{tc}	K_{rc}	K_{te}	K_{re}	K_{ac}	K_{ae}	ρ (mm)	λ (radians)
1	1502.711	872.908	35.214	3.924	158.481	3.351	0.0140	0.271
2	1589.482	711.431	37.896	11.080	164.130	10.613	0.0036	0.175
3	1618.569	771.311	34.878	7.963	194.033	1.208	0.0157	0.072
4	1495.519	826.804	25.149	10.987	230.458	9.450	0.0058	0.229
5	1580.845	834.470	44.899	17.854	213.170	22.224	0.0172	0.459
6	1631.501	855.775	37.878	27.057	255.069	18.392	0.0104	0.185

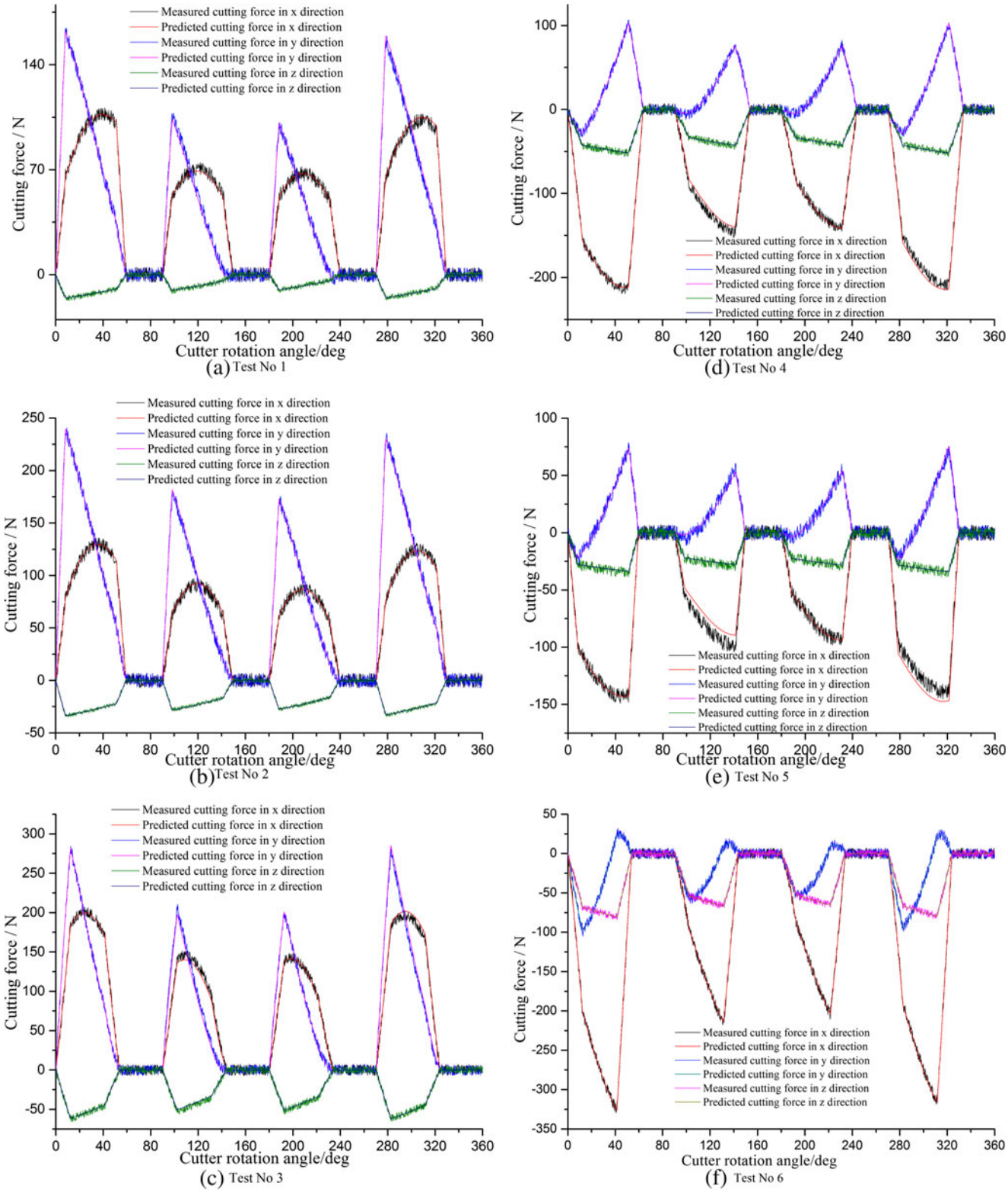

Fig. 7 **a** Comparisons of measured and predicted cutting forces in test no.1. **b** Comparisons of measured and predicted cutting forces in test no. 2. **c** Comparisons of measured and predicted cutting forces in test no. 3. **d** Comparisons of measured and predicted cutting forces in test no. 4. **e** Comparisons of measured and predicted cutting forces in test no. 5. **f** Comparisons of measured and predicted cutting forces in test no. 6

Only using Eq. (14) in test no. 1, we can get the a_1 and b_1 with values 0.0122 and 0.0069. Further, the values of λ and ρ can be obtained with values 0.2709 and 0.0140 based on the Eq. (16). According to the measured and predicted difference values between the cutting force of the first edge and the average cutting force in x and y directions from Fig. 5, the algorithm for the calibrating values of λ and ρ has good fitting results.

$$\begin{cases} \lambda = \arctan\alpha_i + \dfrac{\pi}{N}(2i-3) \\ \alpha_i = \arctan\dfrac{a_i}{b_i} \\ \rho = \dfrac{a_i + b_i}{\sin\alpha_i + \cos\alpha_i} \end{cases} \tag{16}$$

As similar with the calibration of the run-out parameters, we can get the good fitting prediction results from the Eq. (13) without reconstructing coefficient matrix. By substituting the run-out parameters λ and ρ into the Eq. (13) in test no. 1, the calibration values of the axial cutting force coefficients K_{ac} and the axial blade force coefficients K_{ae} can be solved as.177.503 and 2.678. In Fig. 6, it is shown that the calibrating results of average cutting force in z direction are consistent with those of experiments.

On the basis of above study, the two methods should be used to calibrate the force coefficients and run-out parameters. For the cutting force coefficients K_{tc}, K_{rc} and the blade force coefficients K_{te}, K_{re}, the calibration process based on the least square method need to include the average cutting forces information in x and y directions to solve the ill-posed problem. But, for the axial cutting force coefficients K_{ac}, the axial blade force coefficients K_{ae} and run-out parameters λ and ρ, the good fitting prediction result can be achieved only using the one direction cutting forces information without reconstructing coefficient matrix.

3.2 Prediction results of cutting forces

The cutting force graph with the sampling time as the abscissa provided by a dynamometer is translated into the one with the cutter rotation angle as the abscissa, according to the spindle speed and sample frequency. It follows from Sect. 2.3 that the cutting force coefficients can be determined from Eqs. (14) and (15), then the values of ρ and λ can be solved from Eq. (16). The calibrated values of these in the cutting tests are shown in Table 2.

The predicted and measured cutting forces are given in Fig. 7, which are measured from test no.1 to test no. 6. Clearly, the predicted results are of well conformity with the measured cutting forces both in magnitude and in distribution, despite of cutting types and cutting conditions (Fig. 7).

4 Conclusions

In this paper, the calibration accuracy of the cutting force coefficients and the cutter radial run-out parameters in flat-end milling has been discussed. In order to eliminate the influence of the ill-posed problem on calibration accuracy, the cutting force coefficient matrix was optimized by incorporating the average cutting information in x and y directions based on the least square method. The presented identification method is tested and validated by the experimental data.

The main work of this paper can be summarized as follows: first, in order to eliminate the numerical oscillations on the cutting force waveforms and simplify the procedure of calibration, the continuous form of cutting force model and the constant coefficients are used to predict the cutting force; secondly, the ill-posed problem in calibration of the tangential and radial cutting force coefficients was found out, and the solution method was proposed to enhance the calculation stability and to get a useful and stable solution.

Reference

1. Koenigsberger F, Sabberwal AJP (1961) An investigation into the cutting force pulsations during milling operations. Int J Mach Tools Des Res 1(1):15–33
2. Kline WA, DeVor RE (1983) The effect of runout on cutting geometry and forces in end milling. Int J Mach Tools Des Res 23(2):123–140
3. Altintas Y (2000) Manufacturing automation, metal cutting, machine tool vibration and CNC design. CambridgeUniversity Press, Cambridge
4. Lazoglu I (2003) Sculpture surface machining: a generalized model of ball-end milling force system. Int J Mach Tools Manuf 43(5): 453–462
5. Liang SY, Wang JJ (1994) Milling force convolution modeling for identification of cutter axis offset. Int J Mach Tools Manuf 34(8): 1177–1190
6. Wang JJJ, Zheng CM (2003) Identification of cutter offset in end milling without a prior knowledge of cutting coefficients. Int J Mach Tools Manuf 43(7):687–697
7. Melkote SN, EndresbW J (1998) The importance of including size effect when modeling slot milling. J Manuf Sci Eng 120(1):68–75
8. Rivière-Lorphèvre E, Filippi E (2009) Mechanistic cutting force model parameters evaluation in milling taking cutter radial runout into account. Int J Adv Manuf Technol 45:8–15
9. Kao Y-C, Nguyen N-T, Chen M-S, Su S-T (2015) A prediction method of cutting force coefficients with helix angle of flat-end cutter and its application in a virtual three-axis milling simulation system. Int J Adv Manuf Technol 77:1793–1809
10. Wang B, Hao H, Wang M, Hou J, Feng Y (2013) Identification of instantaneous cutting force coefficients using surface error. Int J Adv Manuf Technol 68:701–709
11. Yun W-S, Cho D-W (2000) An improved method for the determination of 3D cutting force coefficients and runout parameters in End milling. Int J Adv Manuf Technol 16:851–858
12. Ko JH, Cho D-W (2005) Determination of cutting-condition-independent coefficients and runout parameters in ball-End milling. Int J Adv Manuf Technol 26:1211–1221

13. Lee T, Lin Y (2000) A 3D predictive cutting-force model for end milling of parts having sculptured surfaces. Int J Adv Manuf Technol l16(11):773–783
14. Wan M, Zhang WH (2006) Calculations of chip thickness and cutting forces in flexible end milling. Int J Adv Manuf Technol 29(7–8):637–647
15. Wan M, Zhang WH, Tan G, Qin GH (2007) New algorithm for calibration of instantaneous cutting-force coefficients and radial run-out parameters in flat end milling. Proc Inst Mech Eng B J Eng Manuf 221(6):1007–1019
16. Yang L, DeVor RE, Kapoor SG (2005) Analysis of force shape characteristics and detection of depth-of-cut variations in end milling. J Manuf Sci Eng 127(3):454–462